

Prevention of Cyanobacterial Blooms Using Nanosilica: A Biomineralization-Inspired Strategy

Wei Xiong,[†] Yiming Tang,[‡] Changyu Shao,[†] Yueqi Zhao,^{†,§} Biao Jin,[†] Tingting Huang,[‡] Ya'nan Miao,[‡] Lei Shu,^{†,§} Weimin Ma,^{*,‡} Xurong Xu,^{*,§} and Ruikang Tang^{*,†}

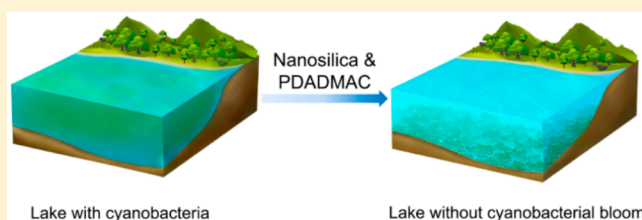
[†]Center for Biomaterials and Biopathways, Department of Chemistry, Zhejiang University, Hangzhou 310027, China

[‡]College of Life and Environmental Science, Shanghai Normal University, Shanghai 200234, China

[§]Qiushi Academy for Advanced Studies, Zhejiang University, Hangzhou 310027, China

S Supporting Information

ABSTRACT: Cyanobacterial blooms represent a significant threat to global water resources because blooming cyanobacteria deplete oxygen and release cyanotoxins, which cause the mass death of aquatic organisms. In nature, a large biomass volume of cyanobacteria is a precondition for a bloom, and the cyanobacteria buoyancy is a key parameter for inducing the dense accumulation of cells on the water surface. Therefore, blooms will likely be curtailed if buoyancy is inhibited. Inspired by diatoms with naturally generated silica shells, we found that silica nanoparticles can be spontaneously incorporated onto cyanobacteria in the presence of poly(diallyldimethylammonium chloride), a cationic polyelectrolyte that can simulate biosilicification proteins. The resulting cyanobacteria-SiO₂ complexes can remain sedimentary in water. This strategy significantly inhibited the photoautotrophic growth of the cyanobacteria and decreased their biomass accumulation, which could effectively suppress harmful bloom events. Consequently, several of the adverse consequences of cyanobacteria blooms in water bodies, including oxygen consumption and microcystin release, were significantly alleviated. Based on the above results, we propose that the silica nanoparticle treatment has the potential for use as an efficient strategy for preventing cyanobacteria blooms.



INTRODUCTION

As primary photosynthetic microorganisms, cyanobacteria are found almost everywhere and have a profound impact on the earth's atmosphere and biosphere.^{1–3} However, cyanobacteria can also reproduce exponentially and uncontrollably, and they die rapidly under certain conditions such as virus infection,^{4,5} which is commonly referred to as a harmful cyanobacterial bloom.^{6,7} The frequency of blooms has increased in water bodies around the world.^{6,7} These blooms produce cyanotoxins that can poison and cause the death of animals and humans,^{8–11} and more importantly, the resulting anaerobic water induces the large-scale death of aerobic organisms, threatens the safety of drinking water, and destroys aquatic ecosystems.^{12,13} For instance, a large-scale cyanobacterial bloom in Taihu Lake (Jiangsu Province, China) led to a highly publicized drinking water crisis in 2007 that affected more than five million people.^{7,13,14} To reduce and hopefully avoid the potential risks associated with cyanobacteria blooms, several approaches have been developed, such as the addition of toxic algacides and flocculants.^{15,16} However, these methods have significant disadvantages, such as secondary pollution, low biological selectivity and adverse environmental impacts.¹⁷ Therefore, developing novel pathways for avoiding cyanobacterial blooms represents a great challenge.

A cyanobacterial bloom is caused by variations in the vertical position of large volumes of cyanobacterial biomass, which develops gradually and accumulates over a long time.¹⁸ In nature, many cyanobacteria have intracellular gas vesicles that make the cells buoyant.^{19–21} The floating characteristic is an important factor in the occurrence of cyanobacterial blooms because buoyant cyanobacteria float upward to accumulate in dense surface blooms.^{19–21} Subsequently, their accelerated death induced by rising temperatures and light intensities, which result in the large-scale consumption of dissolved oxygen and the release of cyanotoxins when huge cyanobacterial cells are hard to disperse within certain time and space.^{8–13} Therefore, the control of buoyant cells is the key to preventing cyanobacterial blooms in advance. Compared with cyanobacteria, diatoms can use their siliceous walls as a ballast to control water column position.^{22,23} Cell walls made of silica (hydrated silicon dioxide) are called frustules.²⁴ Inspired by diatoms, we conceived that cyanobacteria could be encapsulated within silica to confer upon them diatom-like features. It was also found that cyanobacteria with biosilica shells and green algae

Received: June 10, 2017

Revised: August 28, 2017

Accepted: September 26, 2017

Published: September 26, 2017

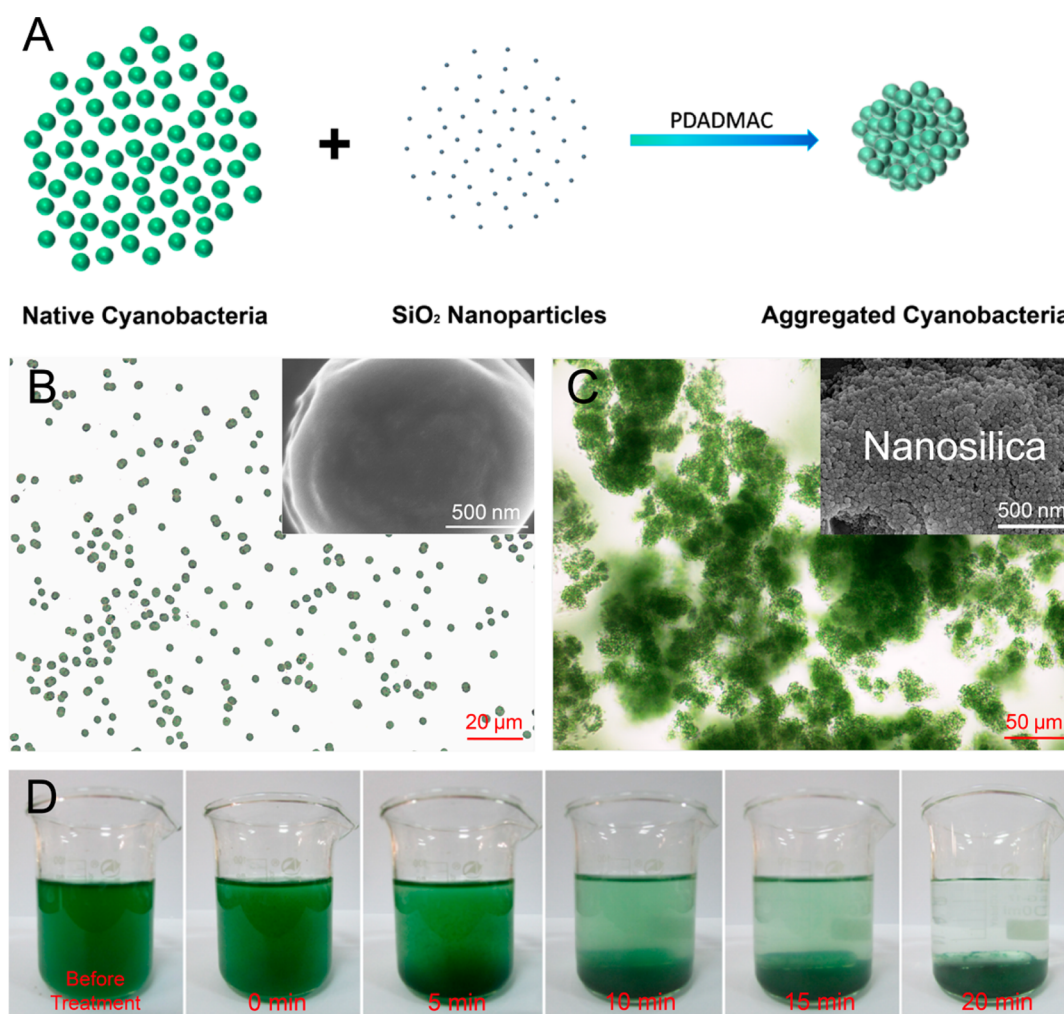


Figure 1. *Microcystis flos-aquae* cells and their aggregates with silica. (A) Scheme of the direct incorporation of silica nanoparticles on the cyanobacteria using PDADMAC. (B) Native cells under an optical microscope and SEM. (C) Aggregated cells under an optical microscope and SEM; the nanosilica particles could be identified readily on the aggregated cell surfaces. (D) Native cells (before treatment) and aggregated cells in the beaker (100 mL) at different times, which demonstrated rapid sedimentation of the cells in the presence of silica and PDADMAC.

aggregates induced by silicification have the tendency to sink to the bottom due to the increased density.^{25,26} Compared with diatoms, the silica-adsorbed cyanobacteria cells can remain in a sedimentary state, thereby inhibiting rapid cell growth and subsequent death and possibly reducing the risks of blooms. However, one challenge is that cyanobacteria cannot inherently generate silica walls. Previous biomineralization research has shown that silica formation by diatoms is induced by polycationic peptides that contain polyamine.^{27,28} Recently, silicification proteins and long-chain polyamines (LCPA) have been reported to mimic biosilicification proteins to induce silica precipitation in vitro.^{29–31} As a cationic polyelectrolyte containing positively charged quaternary amines, poly-(diallyldimethylammonium chloride) (PDADMAC) has been successfully used to improve cell silicification abilities.^{25,26,32,33} Herein, we developed a feasible one-step treatment method of directly incorporating silica nanoparticles onto cyanobacteria using PDADMAC, and this approach can suppress cyanobacterial blooms via tactics that are analogous to those in diatoms.

MATERIALS AND METHODS

Cyanobacterial Cell Culture. In the experiment, *Microcystis flos-aquae* was isolated from Meiliang Bay, Taihu Lake,

China (120°30'N, 31°27'E), a water body that has experienced an increased frequency and intensity of major cyanobacterial blooms in warm seasons in recent years. *Microcystis flos-aquae* cells were cultured at 30 °C in a 500 mL reagent bottle (Schott Duran) containing 400 mL of BG-11 cultivation medium,³⁴ buffered with Tris-HCl (5 mM, pH 8.0) bubbled with 2% (v/v) CO₂ in air (30 mL/min), and subjected to continuous illumination by fluorescent lamps (40 μE·m⁻²·s⁻¹) for 24 h (OD₇₃₀ = 0.2–0.3). The chlorophyll *a* concentration was determined spectrophotometrically in methanol.^{35,36}

Silica-Induced Cell Sedimentation. In the experiment, commercially available silica nanoparticles (Ludox TM-40 colloidal silica, diameter (26 ± 4) nm, 40 wt % suspension in water, purchased from Sigma–Aldrich, Saint Louis, MO) were diluted to 5 g/L in NaCl solution (0.02 M). Aqueous NaCl solution (0.02 M) was also used to prepare a 1 g/L poly(diallyldimethylammonium chloride) (PDADMAC, Mw < 100 000 Da, Sigma-Aldrich, Saint Louis, MO) solution. The premade silica nanoparticle suspension in water was first added to the cyanobacteria cell suspension at a concentration of 75 mg/L. After the silica nanoparticles were dispersed in the cell suspension, the PDADMAC solution was added to the cell suspension at a concentration of 2.5 mg/L. Once the

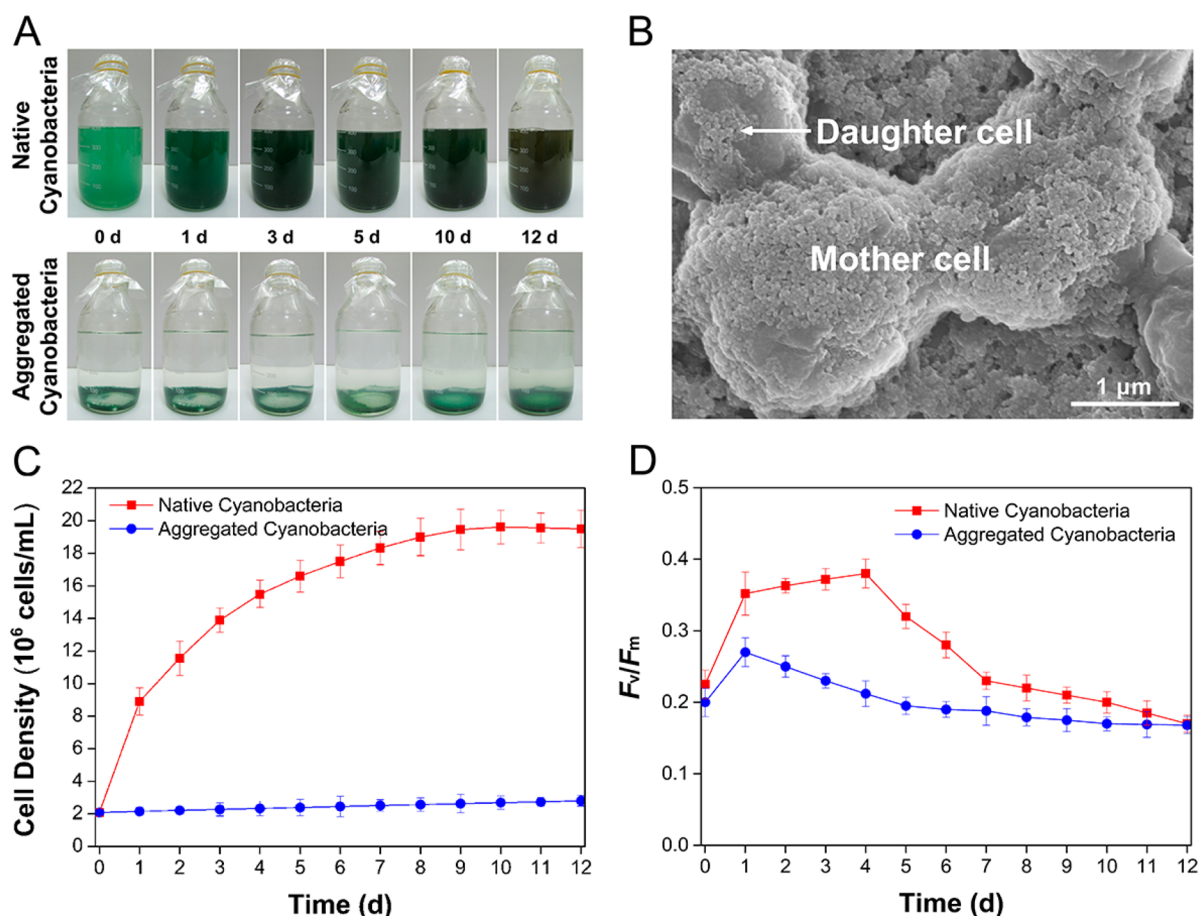


Figure 2. Effect of sedimentation induced by the incorporation of silica on photoautotrophic growth. (A) Photographs of native and aggregated cyanobacteria in culture bottles. (B) SEM of cyanobacterial cells during proliferation; the daughter cells were also spontaneously covered by silica. (C) Cell densities of native and aggregated cyanobacteria ($n = 5$). (D) Photosynthetic activity (F_v/F_m) of native and aggregated cyanobacteria ($n = 5$).

PDADMAC solution was added to the cell suspension, the cells began to aggregate and settle.

Characterizations. Optical microscopy was performed with an Eclipse 50i microscope (Nikon, Japan). Scanning electron microscopy was performed with an S-4800 (Hitachi, Japan) equipped with an energy-dispersive spectroscope (EDAX, USA). The energy-dispersive spectroscope mapping was performed on tinfoil using an accelerating voltage of 20 kV. The size distribution was measured by a Beckman Coulter LS 13320 laser particle size analyzer (Beckman Coulter) using water as the solvent. The zeta potentials of native cyanobacterial cells, silicified cyanobacterial cells and SiO_2 nanoparticles were determined using a Zetasizer Nano S (Malvern, UK). The cell densities of native cyanobacterial cells and silicified cyanobacterial cells were approximately 2×10^5 cells/mL in 10 mM PBS buffer (pH 7.0) during testing.

Chlorophyll Fluorescence Analysis. The chlorophyll fluorescence yields in the steady state of electron transport were measured using a Dual-PAM-100 monitoring system (Walz, Effeltrich, Germany) equipped with an ED-101US/MD unit.^{37,38} The minimal fluorescence at the open photosystem II (PSII) centers in the dark-adapted state (F_0) was excited by a weak measuring light (650 nm) at a PFD of 0.05 to 0.15 $\mu\text{E} \cdot \text{m}^{-2} \cdot \text{s}^{-1}$. A saturating pulse of red light (600 ms, 10,000 $\mu\text{E} \cdot \text{m}^{-2} \cdot \text{s}^{-1}$) was applied to determine the maximal fluorescence at the closed PSII centers in the dark-adapted state (F_m). The

maximal quantum yield of PSII (F_v/F_m) was evaluated as $(F_m - F_0)/F_m$.³⁹

Oxygen Concentration Measurement. The oxygen concentration in the cell suspension was measured with custom-made microsensors.^{40,41} The O_2 microsensor was an OX-MR microsensor (Unisense, Denmark), and the tip diameter was 400–600 μm . The O_2 concentration in the cyanobacterial cell suspension was detected by dipping the O_2 microsensor into the suspension.

Microcystin Analysis. The initial concentration of cyanobacteria (measured in terms of the concentration of chlorophyll *a*) in the water was 1.1 mg/L. Laboratory experiments were performed in triplicate in a 500 mL reagent bottle (Schott Duran) containing 400 mL of BG-11 cultivation medium with cyanobacterial cells at $30(\pm 1)^\circ\text{C}$ under continuous illumination ($50 \mu\text{E} \cdot \text{m}^{-2} \cdot \text{s}^{-1}$ and $500 \mu\text{E} \cdot \text{m}^{-2} \cdot \text{s}^{-1}$) from fluorescent lamps (Narva). The solid biomass of the cyanobacteria was removed via filtration through a GF/C Whatman filter, and the concentration of extracellular microcystins (MCs) in the solution was determined by a highly sensitive double antibody sandwich enzyme-linked immunosorbent assay (ELISA) method (LOD = 0.1 μg MC/L). More experimental details are provided in the [Supporting Information \(SI\)](#).

■ RESULTS AND DISCUSSION

Microcystis spp. is one of the most frequently encountered cyanobacteria in freshwater bodies, and it dominates cyanobacterial blooms in water bodies.^{42,43} The life cycle of *Microcystis* that forms bloom can be divided as different phases, from dormancy, recruitment, growth and floating to the water surface. *Microcystis* spp. can use gas vesicles to vary their buoyancy to obtain favorable growth conditions,¹⁸ and these organisms produce hepatotoxins known as MCs.⁴² In this study, we used *Microcystis flos-aquae* as an example to demonstrate the method of incorporating silica onto cyanobacteria cells via PDADMAC (Figure 1A). Under culture conditions, the cells were typically in a unicellular state at 2–3 μm in diameter, and they were suspended evenly throughout the culture medium (Figure 1B; SI Figure S1) and had a surface potential of -12 mV (SI Figure S2). Under scanning electron microscopy (SEM), the native cyanobacterial cells appeared as spheres with smooth surfaces (Figure 1B). Because native cyanobacteria lack silicification proteins or polypeptides, such as silicateins or silaffins, they cannot inherently induce silica deposition or incorporation. Therefore, direct mixing of silica nanoparticles (20–30 nm, 75 mg/L) with the *Microcystis flos-aquae* suspension did not result in silica deposition onto the cells (SI Figures S3, S4, and S5). However, the presence of PDADMAC (2.5 mg/L) immediately induced the coaggregation of cyanobacteria and silica, and the resulting aggregates had typical diameters ranging from 10–100 μm (Figure 1C; SI Figure S1). The adsorbed silica nanoparticles could be observed on the cell surfaces under SEM, which was also confirmed by energy-dispersive X-ray (EDX) spectroscopy (Figure 1C; SI Figure S6 and S7). The element mapping images indicated that the cells cohered with each other via the silica phase in the aggregates. Moreover, the surface potential of each silica-incorporated cyanobacteria was reduced to -3 mV (SI Figure S2), and the lower electrostatic repulsion favored particle agglomeration.^{44–48} Because of the relatively high specific gravity (2.2 g/cm³) of silica, the aggregates sank to the beaker bottom within 20 min (Figure 1D) in our experiments. However, the native cyanobacteria could remain suspended in water uniformly and stably (SI Figure S8).

The cyanobacterial blooms are directly related to the photoautotrophic growth of cells. Generally, the rapid photoautotrophic growth of cyanobacteria and their subsequent death within a limited area could yield conditions detrimental to surrounding biota. To investigate the effects of incorporating silica on the photoautotrophic growth of the cyanobacteria, we placed the native and aggregated (with silica) cells in an optimal cultivation environment (light intensity of $40\text{ }\mu\text{E}\cdot\text{m}^{-2}\cdot\text{s}^{-1}$ and temperature of $30\text{ }^{\circ}\text{C}$). The initial cell density was $2.0 \times 10^6\text{ cells/mL}$ and the suspension color was light green. During the experiment, the native cyanobacteria suspension gradually darkened and gradually darkened indication rapid grew to brown late in the culture within 12 days (Figure 2A), indicating the rapid cell proliferation. However, the aggregated cyanobacteria stayed at the culture bottle bottom and the solution remained clear. This was most likely because cyanobacterial cell growth requires energy produced via photosynthesis, and the reduced total photosensitive area after cell aggregation-sedimentation decreased the level of photosynthesis in the system. Furthermore, the newly generated cells were also coated with silica nanoparticles (Figure 2B) because of the presence of silica and PDADMAC in the solution; therefore, all

of the cells could remain in a sedimented state, which demonstrated the advantage of the one-step solution treatment. Compared with the previous programmed silicification approaches,^{30–33} the current method does not require any complicated treatments and can result in the spontaneous incorporation of SiO_2 on both the original and proliferated cells. This characteristic is important because it can simplify the material-based transformation from cyanobacterial cells to diatom-like cells. Furthermore, the SiO_2 -incorporated cyanobacterial cells are superior to natural diatoms from the perspective of bloom control because natural diatoms utilize silica frustules to vary their depth in water to reach more favorable growth conditions,⁴⁹ whereas the SiO_2 -incorporated cyanobacterial cells always sink to the water bottom and experience slowed photoautotrophic growth.

Cell density is an important parameter that can indicate the photoautotrophic growth of cyanobacterial cells and quantitatively express the degree of the cyanobacterial bloom event. In practice, the key to controlling blooms is controlling the cyanobacterial cell densities. In the above-mentioned experiments, the cell density increased rapidly and the average specific growth rate was approximately 0.61 d^{-1} until day 10 (Figure 2C) for the native cyanobacteria, which indicated large-scale proliferation and was consistent with the chlorophyll *a* (Chl *a*) results (9.8 mg/L, SI Figure S9). The synchronous drop of cell density and Chl *a* content after day 10 indicated that the cells began to die (Figure 2C; SI Figure S9), which might have been caused by senescent and death in the system. However, in the case of aggregated cyanobacteria, the increase in cell density was significantly inhibited and the specific growth rate was relatively stable at the value of $2.25 \times 10^{-2}\text{ d}^{-1}$ throughout the entire experimental period (Figure 2C). This proliferation rate was almost negligible compared with that of the native cyanobacterial cells, which may have been related to the limited growth caused by cell aggregation and the shell material.³³ In addition, increases in the Chl *a* content were also inhibited because the proliferation rate was maintained at only $0.25\text{ mg}\cdot\text{L}^{-1}\cdot\text{d}^{-1}$ (SI Figure S9), which indicated that cell death did not occur. These experimental results demonstrate the efficient inhibition of cell proliferation and photoautotrophic growth in the sedimentary state with the presence of silica and PDADMAC.

Since the treatment protocol requires the materials of silica and PDADMAC, an evaluation of their toxicities is of importance. The results showed that although a large amount of PDADMAC might cause a drop in the biomass (SI Table S1), either silica alone or the combination of silica and PDADMAC did not cause any decrease in the biomass (SI Table S1). It followed that the enrollment of silica can improve the biocompatibility of the treatment and can even eliminate the toxicity of PDADMAC to *Microcystis*. It was also found that silica and PDADMAC at current concentration produce little accompanying toxicity to other ecotoxicologically representative organisms such as *Desmodesmus subspicatus*, *Lemna minor*, *Daphnia magna*, Zebrafish embryos (SI Table S2–S5). Thus, the treatment by the combination of silica and PDADMAC is biologically friendly.

In photosynthetic microorganisms, photosynthetic activity is one of the most important factors for photoautotrophic growth, which plays a dominant role in cyanobacterial bloom formation. F_v/F_m is commonly used as an indicator of photosynthetic activity;^{32,33} and its value in the native cyanobacteria was 0.23 at the beginning of the experiment but increased to 0.33 within 1

day, and this high level was maintained over the following 2–3 days (Figure 2D). The increased photosynthetic activity was mainly attributed to the rapid photoautotrophic growth and cell proliferation of the cyanobacteria, which was consistent with the examined Chl *a* profile (SI Figure S9). Subsequently, the F_v/F_m decreased to 0.17. Because obvious decreases in cell density were not observed as the Chl *a* content rapidly decreased (Figure 2C; SI Figure S9), the decrease in F_v/F_m was most likely because of large-scale cell senescence and death. After cell aggregation, the F_v/F_m value had a slight drop, because the cells inside would be shielded by outside cells from the light, which was in accord with our previous work.²⁶ However, F_v/F_m remained at 0.2 (Figure 2D), indicating inhibited cyanobacterial photoautotrophic growth and cell proliferation. Moreover, it appeared that cell death was not obvious in the aggregated case, which is important for preventing some harmful effects of the blooms.

The above experimental results confirmed that sedimentation induced by the incorporation of silica could effectively inhibit the photoautotrophic growth of cyanobacterial cells, which is significant for preventing harmful blooms of cyanobacteria, which damage water quality by decreasing oxygen supplies and releasing MCs.

The oxygen concentration in an aquatic system is a key index that is closely related to the survival state of cyanobacteria and other aerobic organisms. Die-off of cyanobacterial blooms always depletes oxygen within lakes where huge biomass accumulates and is hard to disperse within certain time and space,^{12,13} and our experiment also confirmed this serious threat. Initially, the O_2 concentration in both the native and aggregated cyanobacteria cell suspensions was approximately 225 $\mu\text{mol/L}$ (Figure 3A; SI Figure S10), and this value was similar to the O_2 saturation concentration ($\sim 226 \mu\text{mol/L}$) in the culture medium at room temperature. Although the rapid proliferation of the native cells could increase cell density to promote O_2 production at the initial state (SI Figure S10), a large amount of O_2 in the suspension was consumed only after 1 day (SI Figure S10). Due to the increasing cell respiration, the O_2 concentration in the suspension became to reduce significantly and at day 12, dropped to 180 $\mu\text{mol/L}$ (Figure 3A; SI Figure S10). At day 20, the O_2 concentration had further reduced to 10 $\mu\text{mol/L}$ (Figure 3A), which indicated that the aquatic system had become oxygen deficient because of the rapid proliferation and subsequent death of the cells, which both consume O_2 . However, the O_2 concentration in the aggregated cyanobacteria cell suspension was nearly unchanged and remained at the O_2 saturation concentration (Figure 3A) primarily because of the restrained photoautotrophic growth in the sedimentary state. The restrained cell growth led to slow cell senescence, which promoted slower oxygen consumption and allowed the oxygen consumption by the cells and the oxygen dissolution from the air to reach a dynamic equilibrium. Therefore, the silica-induced cell aggregation and sedimentation did not cause additional biological O_2 consumption, and the ecological balance in the bottle remained at a healthy state.

MCs released by *Microcystis* spp. represent another harmful factor for water quality because of their potentially fatal effects, such as liver damage, nephrotoxicity and neurotoxicity.^{50–52} In our experiments, the concentration of MCs was examined by the highly sensitive ELISA method. In the native cyanobacterial system, the release of MCs accelerated as the experiment continued at a rate of approximately $0.04 \mu\text{g}\cdot\text{L}^{-1}\cdot\text{d}^{-1}$ (Figure 3B) because of the rapid cell proliferation and senescence. On

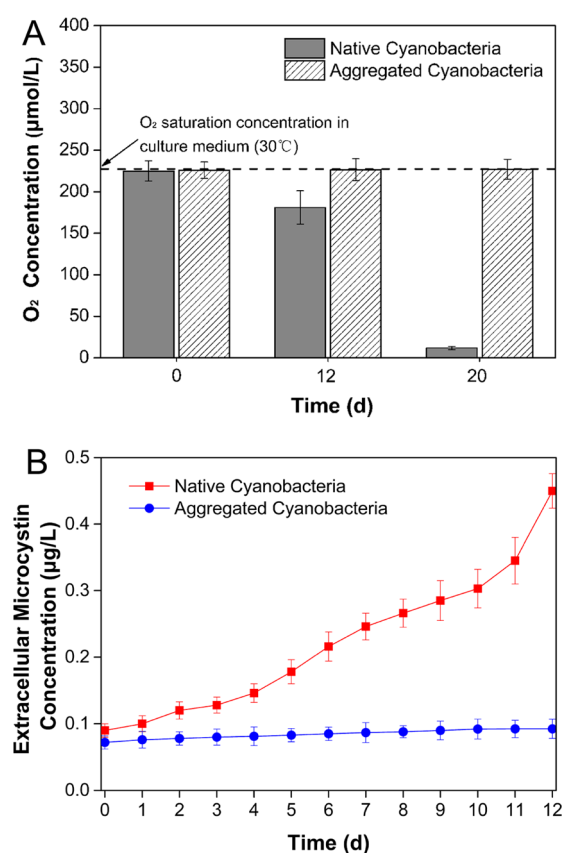


Figure 3. Comparison of water quality parameters in the optimal cultivation environment. (A) Oxygen concentration in the culture medium of native and aggregated cyanobacteria ($n = 5$). (B) Extracellular microcystin concentration of native and aggregated cyanobacteria ($n = 5$).

day 12, the MC concentration in the water reached $0.45 \mu\text{g}\cdot\text{L}^{-1}$, which was considerably higher than the initial value of $0.07 \mu\text{g}\cdot\text{L}^{-1}$, and the rate of MC release increased rapidly, which was likely due to rupture of the cell membrane in cell death. However, the extracellular concentration of MCs in the water system was not affected by the aggregated cyanobacteria, and even after 12 days, the concentration was limited to within $0.08 \mu\text{g}\cdot\text{L}^{-1}$ because photoautotrophic growth was mostly inhibited in the sedimentary state, which slowed cell senescence and death.

All of the above results demonstrate that the presence of silica and PDADMAC can effectively inhibit the large-scale proliferation and death of cyanobacteria, thereby protecting water quality. The key factor appears to be cell sedimentation. In natural aquatic systems, the lake bed is relatively dark and a lower, more constant water temperature is maintained compared with that at the lake surface, and these conditions can further inhibit the proliferation of cyanobacteria. Our extended experiment confirmed that cell growth and the MC release rate were suppressed when the aggregated cyanobacteria were placed under low temperature (4°C) conditions (SI Figures S11 and S12). Moreover, cyanobacterial blooms are less likely to occur in winter because of the low temperatures and light intensity. Because sedimentation can create low temperatures and low light intensity, the described treatment may prevent cyanobacterial blooms more efficiently in nature than in the laboratory. Because cyanobacteria aggregates may still suspend in natural aquatic systems because of water flow, we

also investigated the effect of our treatment on the photo-autotrophic growth and MC release rate of the aggregated cyanobacteria under intense light conditions (light intensity: $500 \mu\text{E}\cdot\text{m}^{-2}\cdot\text{s}^{-1}$; temperature: 30°C) (SI Figures S13 and S14), and a significant preventive effect was still observed.

The influential factors for the cell-material aggregation formation and the sedimentation were examined. We investigated the cell aggregation and sedimentation under the conditions with different PDADMAC concentrations. The optimum PDADMAC concentration was 2.5 mg/L and the total sedimentation time was about 20 min when SiO_2 concentration was 75 mg/L ; any change (decreasing or increasing) of the amount in the system (0.5, 1.0, 5.0, and 10.0 mg/L) would lead to the extended time for sedimentation (SI Figure S15 and Table S6). Other kinds of cationic polyelectrolyte containing positively charged amines, such as poly(allylamine hydrochloride) (PAH) and poly(ethylenimine) (PEI), were also effective on the cell treatment but their effects were different (SI Figure S16 and Table S7). Of these polyelectrolytes, PDADMAC was always most effective in cell removal. It should be mentioned that the polyelectrolytes with low molecular weight were superior to those with high molecular weight (SI Figure S16 and Table S7). SiO_2 was another key factor in the coaggregation and sedimentation treatment. Increasing SiO_2 amount in the treatment would always promote cell aggregation and sedimentation and the concentration range was $0\text{--}150 \text{ mg/L}$. Although PDADMAC alone could induce cell aggregation, it could not result in any rapid sedimentation without SiO_2 (SI Figure S17 and Table S8). By using 150 mg/L SiO_2 and 2.5 mg/L PDADMAC, all the cyanobacterial cells could sink to the bottom within 10 min (Supporting Information, Figure S17 and Table S8). However, further increasing SiO_2 had no effect on settling periods (SI Figure S17 and Table S8). We also found that total sedimentation time reduce gradually with the increase of temperature in the range of $4\text{--}42^\circ\text{C}$, from 60 min at 4°C to 10 min at 42°C (SI Figure S18 and Table S9). The fluctuation of solution pH ($5.5\text{--}8.5$) had no effect on the coaggregation and the sedimentation, and the settling periods were about 20 min (SI Figure S19 and Table S10). However, extremely low pH (<4.0) or high pH (>10.5) would extend total sedimentation time (SI Figure S19 and Table S10). Furthermore, our tests demonstrated the validity of the treatment for different cell densities of *Microcystis flos-aquae* (1.2×10^6 , 3.6×10^6 , 7.2×10^6 and 2.0×10^7 cells/mL), many other cyanobacteria (*Microcystis flos-aquae*, *Microcystis aeruginosa*, *Anabaena* sp. strain PCC 7120, *Synechococcus elongatus* PCC 7942 and *Synechocystis* sp. strain PCC 6803) (SI Figures S20 and S21, Tables S11 and S12), as well as *Microcystis* colonial cells and green algae (SI Figure S21 and Table S12).

In order to extend the study, we collected water samples from Taihu Lake (30 cm below the surface) in the cyanobacteria bloom season to investigate whether the treatment was effective in natural water samples. The cell density of the original water sample was approximately 0.8×10^6 cells/mL. After the treatment, the cell density in the supernatant was less than 1.0×10^4 cells/mL. We placed the original water sample and the treated water sample in an optimal cultivation environment (light intensity: $40 \mu\text{E}\cdot\text{m}^{-2}\cdot\text{s}^{-1}$; temperature: 30°C) with light-dark transitions (light: 12 h; dark: 12 h). The cells in the original water sample without any treatment remained in a suspended state for 2 to 3 days, and the water sample was always turbid. In addition, the color of the

water sample changed from light green (initial color) to light yellow (final color) and the biomass content (expressed as Chl *a* content) began to decrease after 1 day (Figure 4), which

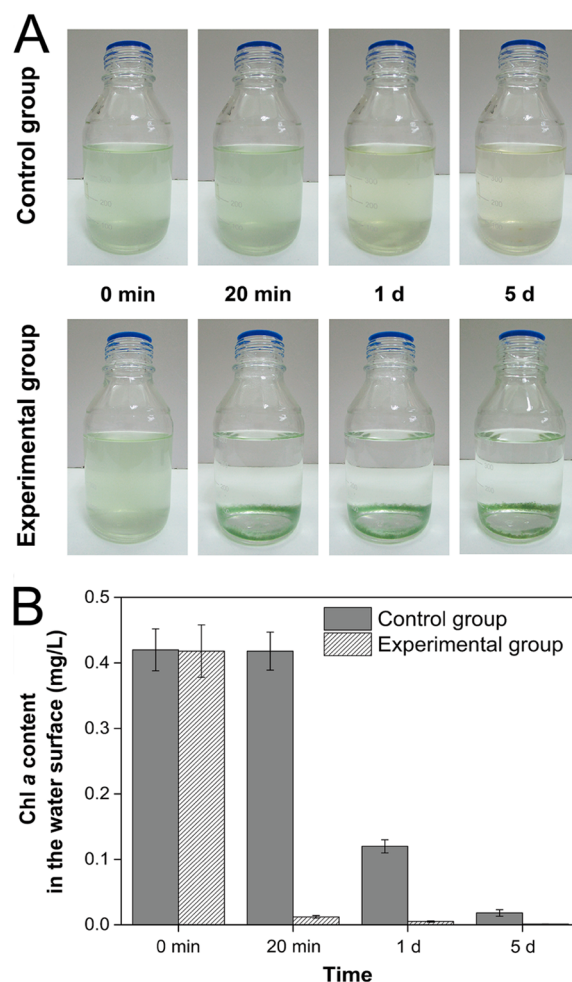


Figure 4. Effect of the treatment on the natural water sample in the optimal cultivation environment with light-dark transitions. (A) Photographs of original and treated water sample in culture bottles. (B) Chlorophyll *a* content of original and treated water sample from the surface layer ($n = 5$). Control group: the original water sample collected from Taihu lake without any treatment; experimental group: the original water sample collected from Taihu lake treated by silica and PDADMAC (0 min: the water sample before treatment). The water sample was 400 mL in the 500 mL reagent bottle (Schott Duran).

indicated that the cells gradually died. This finding differed from the results observed in the laboratory culture (Figure 2A; SI Figure S13a) but was nearly consistent with the results for the native cyanobacterial blooms, which was primarily because fewer nutrients are available in the natural lake water than in the culture medium. However, after the natural lake water was subjected to the silica and PDADMAC treatments, the cells quickly aggregated and sank to the bottle bottom within 20 min (Figure 4A); moreover, the cell density of the supernatant remained less than 1.0×10^4 cell/mL and the Chl *a* content in the supernatant decreased to zero at 5 days (Figure 4B), which confirmed that the sedimentary state was well maintained. Moreover, the water became clear and transparent after the treatment, indicating that the silica nanoparticles and

PDADMAC have the potential for use as water clarifying agents.

A field test was performed in a natural pond in XiXi Wet Land, Hangzhou, Zhejiang Province, China. The pond storage was 10 m³, and original algal cell density was approximately 5.0×10^5 cells/mL (SI Figure S22), including about 3.0×10^5 cells/mL of cyanobacteria and 2.0×10^5 cells/mL of green algae (SI Figure S23). Before treatment, the surface of the pond was green and turbid (Figure 5A), and the water sample

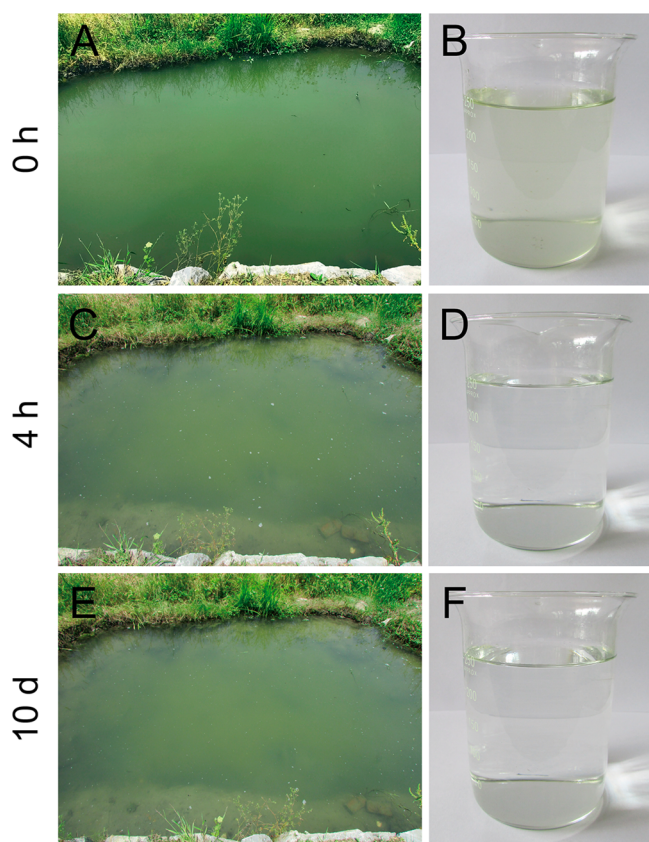


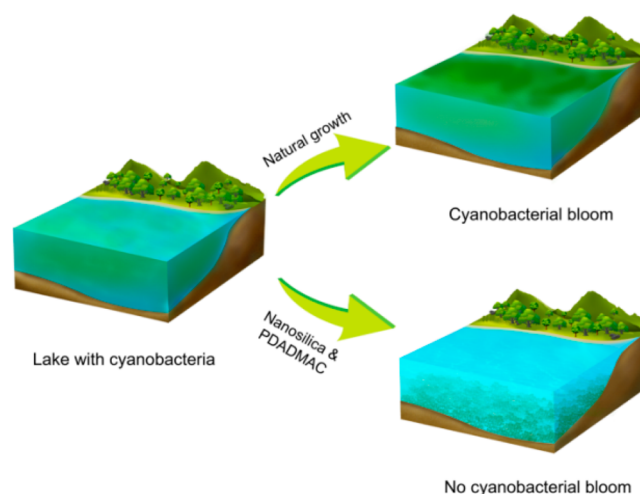
Figure 5. Effect of the treatment on the natural water body. (A) Photograph of a pond without any treatment. (B) Original water sample collected from the pond without any treatment in 250 mL beaker. (C) Photograph of the pond treated by silica and PDADMAC at 4 h. (D) Water sample collected from the pond treated by silica and PDADMAC at 4 h in 250 mL beaker. (E) Photograph of the pond treated by silica and PDADMAC at day 10. (F) Water sample collected from the pond treated by silica and PDADMAC at day 10 in 250 mL beaker.

(collected 30 cm below the surface) was light green (Figure 5B). When the pond water was treated by silica (75 mg/L) and PDADMAC (2.5 mg/L), the cells quickly aggregated and sank to the bottom within 4 h, and the water became limpid (Figure 5C). The water sample collected from the pond was clear and transparent (Figure 5D); and the algal cell density of the water sample was reduced to about 4.0×10^4 cells/mL (SI Figure S22). Moreover, the clarified state of the pond could be maintained well after the treatment, both the water in the pond and the collected water sample kept in the clear state at day 10 (Figure 5E and F), and the algal cell density was further reduced to 1.5×10^4 cells/mL (SI Figure S22). After 10 days, the algal cell densities of the water sample from the pond began to increase slightly, but the density was controlled within $1.8 \times$

10^5 cells/mL at day 20 (SI Figure S22). The F_v/F_m parameter in the sedimentary and aggregated populations declined from initial 0.35 to 0.12 at day 15 and recovered to 0.18 at day 20 (SI Figure S24), suggesting that there were still slow growth. And bottom dissolved oxygen (DO) declined from initial 5.8 mg/L to 5.0 mg/L at day 15 and increased to 5.2 mg/L at day 20 (SI Figure S25), which was in accordance with the F_v/F_m profile in the sedimentary and aggregated populations. In addition, we also found that the small fishes in the pond were not affected by the treatment and all kept well without any change. It should be emphasized that this field treatment was performed under completely natural condition, validating laboratory results.

Cyanobacterial blooms are known to have a significant impact on human health and aquatic ecosystems. Although the control of cyanobacterial blooms has been acknowledged as an important component in the management of public drinking, agricultural, and recreational water supplies, an effective method of preventing these blooms has not been developed. Currently, mechanical treatments of cyanobacterial blooms using nontoxic natural clay represents a promising approach; however, natural clay was inefficient in the removal of algae cells in comparison with silica nanoparticles due to its poor colloidal property, and such processes require massive amounts of clay (250 mg/L), which complicates field applications.^{53–55} And the rapid development of material sciences has opened new pathways for managing cyanobacterial blooms that emphasize the killing of cyanobacteria or the removal of cyanotoxins via nanomaterials, such as zerovalent iron and N-doped titanium dioxide.^{14,56} Different from the above technologies, our attempt provides an alternative bioinspired strategy for preventing cyanobacterial blooms in natural aquatic systems (Scheme 1). According to our laboratory and field

Scheme 1. Silica-Induced Cell Sedimentation for the Prevention of Cyanobacterial Bloom



tests, when the concentration of bloom comes up to $10^5 \sim 10^6$ cells/mL and the season is the end of spring and the beginning of summer, with single addition of silica and PDADMAC, this technique will give optimal effect. Moreover, the concentrations of PDADMAC and silica materials utilized for this approach are only 2.5 and 75 mg/L, respectively. In addition, the inorganic material of silica is a common mineral in the earth and it also serves as an important biomineral in many aquatic organisms,^{58–62} and PDADMAC is an organic material similar

to a silicification protein. These applied materials are biocompatible and environmentally friendly. Furthermore, the commercial silica nanoparticles and PDADMAC are available in markets and the estimated material cost for the water treatment can be controlled within \$0.6 per m³ water, which can ensure its application with little expense. Therefore, the current method is recommended for its ecological benefits and economic feasibility. The spontaneous incorporation of silica on the cyanobacteria in the presence of PDADMAC can effectively prevent cyanobacterial blooms because of the sedimentation effect, which implies a material-based evolution from cyanobacteria to a diatom-like organism via the biomimetic approach. This approach may be extended to many more living organisms, thus highlighting a novel biomineralization-inspired strategy in organism improvement via functional materials and indicating their potential use in ecological controls.⁵⁷

■ ASSOCIATED CONTENT

■ Supporting Information

The Supporting Information is available free of charge on the ACS Publications website at DOI: 10.1021/acs.est.7b02985.

Additional information as noted in the text (PDF)

■ AUTHOR INFORMATION

Corresponding Authors

* (R. T.) Phone: +86 571 87953736; fax: +86 571 87953736; e-mail: rtang@zju.edu.cn.

*(W. M.) +86 21 64321617; fax: +86 21 64321617; e-mail: wma@shnu.edu.cn.

*(X. X.) E-mail: xxu@zju.edu.cn.

ORCID

Xurong Xu: 0000-0002-0626-0597

Ruikang Tang: 0000-0001-5277-7338

Author Contributions

R.T., X.X., and W.M. conceived of the project; W.X., W.M., and R.T. designed the research; W.X. devised the cell aggregation methods; W.X., Y.T., and Y.M. contributed to the cell culture and measurements of O₂ concentration; W.X., C.S., B.J., Y.Z., and L.S. completed the sample characterizations; W.X. and T.H. performed the measurements of the Chl *a* contents and microcystin concentrations; W.X. and L.S. completed the field test. W.X., W.M., X.X., and R.T. performed the data analyses; and W.X., W.M., and R.T. wrote the manuscript.

Notes

The authors declare no competing financial interest.

■ ACKNOWLEDGMENTS

We gratefully acknowledge the support of the Fundamental Research Funds for the Central Universities (ZJU President Project). This work was also supported by the National Natural Science Foundation of China (21471129 and 31370270). Dr. W. Xiong was supported by the Excellent Doctoral Student Supporting Program of Zhejiang University. We thank F. Chen (Department of Chemistry, Zhejiang University, Hangzhou, China) and J. Wang (State Key Laboratory of Silicon Materials, Zhejiang University, Hangzhou, China) for their assistance in the scanning electron microscopy analyses. We also thank Dr. H. Pan (Qiushi Academy for Advanced Studies, Zhejiang University, Hangzhou, China), Dr. X. Wang (Qiushi Academy for Advanced Studies, Zhejiang University, Hangzhou, China),

Dr. Z. Liu (Department of Chemistry, Zhejiang University, Hangzhou, China), and R. Zhao (Department of Chemistry, Zhejiang University, Hangzhou, China) their advice. This research was supported by the Fundamental Research Funds for the Central Universities (ZJU President Project) and the National Natural Science Foundation of China (21471129 and 31370270).

■ ABBREVIATIONS

PDADMAC	poly(diallyldimethylammonium chloride)
Chl <i>a</i>	chlorophyll <i>a</i>
MC	microcystin
ELISA	enzyme-linked immunosorbent assay

■ REFERENCES

- (1) Kump, L. R.; Barley, M. E. Increased subaerial volcanism and the rise of atmospheric oxygen 2.5 billion years ago. *Nature* **2007**, *448* (7157), 1033–1036.
- (2) Rasmussen, B.; Fletcher, I. R.; Brocks, J. J.; Kilburn, M. R. Reassessing the first appearance of eukaryotes and cyanobacteria. *Nature* **2008**, *455* (7216), 1101–1104.
- (3) Anderson, D. M.; Glibert, P. M.; Burkholder, J. M. Harmful algal blooms and eutrophication: Nutrient sources, composition, and consequences. *Estuaries* **2002**, *25* (4), 704–726.
- (4) Manage, P. M.; Kawabata, Z.; Nakano, S. Seasonal changes in densities of cyanophage infectious to *Microcystis aeruginosa* in a hypereutrophic pond. *Hydrobiologia* **1999**, *411*, 211–216.
- (5) Brussaard, C. P. Viral control of phytoplankton populations—a review. *J. Eukaryotic Microbiol.* **2004**, *51* (2), 125–138.
- (6) Paerl, H. W.; Huisman, J. Blooms like it hot. *Science* **2008**, *320* (5872), 57–58.
- (7) O'neil, J. M.; Davis, T. W.; Burford, M. A.; Gobler, C. J. The rise of harmful cyanobacteria blooms: the potential roles of eutrophication and climate change. *Harmful Algae* **2012**, *14*, 313–334.
- (8) Funari, E.; Testai, E. Human health risk assessment related to cyanotoxins exposure. *Crit. Rev. Toxicol.* **2008**, *38* (2), 97–125.
- (9) Cox, P. A.; Banack, S. A.; Murch, S. J.; Rasmussen, U.; Tien, G.; Bidigare, R. R.; Metcalf, J. S.; Morrison, L. F.; Codd, G. A.; Bergman, B. Diverse taxa of cyanobacteria produce β-N-methylamino-L-alanine, a neurotoxic amino acid. *Proc. Natl. Acad. Sci. U. S. A.* **2005**, *102* (14), 5074.
- (10) Cox, P. A.; Banack, S. A.; Murch, S. J. Biomagnification of cyanobacterial neurotoxins and neurodegenerative disease among the Chamorro people of Guam. *Proc. Natl. Acad. Sci. U. S. A.* **2003**, *100* (23), 13380–13383.
- (11) Ding, W. X.; Shen, H. M.; Ong, C. N. Microcystic cyanobacteria extract induces cytoskeletal disruption and intracellular glutathione alteration in hepatocytes. *Environ. Health Persp.* **2000**, *108* (7), 605–609.
- (12) Pu, P.; Hu, W. P.; Yan, J.; Wang, G.; Hu, C. A physico-ecological engineering experiment for water treatment in a hypertrophic lake in China. *Ecol. Eng.* **1998**, *10* (2), 179–190.
- (13) Qin, B.; Zhu, G.; Gao, G.; Zhang, Y.; Li, W.; Paerl, H. W.; Carmichael, W. W. A drinking water crisis in Lake Taihu, China: linkage to climatic variability and lake management. *Environ. Manage.* **2011**, *45* (1), 105–112.
- (14) Xu, H.; Paerl, H. W.; Qin, B.; Zhu, G.; Hall, N. S.; Wu, Y. Determining critical nutrient thresholds needed to control harmful cyanobacterial blooms in eutrophic Lake Taihu, China. *Environ. Sci. Technol.* **2014**, *49* (2), 1051–1059.
- (15) Dixon, M. B.; Richard, Y.; Ho, L.; Chow, C. W. K.; O'Neill, B. K.; Newcombe, G. Integrated membrane systems incorporating coagulation, activated carbon and ultrafiltration for the removal of toxic cyanobacterial metabolites from *Anabaena circinalis*. *Water Sci. Technol.* **2011**, *63* (7), 1405–1411.
- (16) Chow, C. W.; Drikas, M.; House, J.; Burch, M. D.; Velzeboer, R. M. The impact of conventional water treatment processes on cells of

the cyanobacterium *Microcystis aeruginosa*. *Water Res.* **1999**, *33* (15), 3253–3262.

(17) Marsalek, B.; Jancula, D.; Marsalkova, E.; Mashlan, M.; Safarova, K.; Tucek, J.; Zboril, R. Multimodal action and selective toxicity of zerovalent iron nanoparticles against cyanobacteria. *Environ. Sci. Technol.* **2012**, *46* (4), 2316–2323.

(18) Kong, F. X.; Gao, G. Hypothesis on cyanobacteria bloom-forming mechanism in large shallow eutrophic lakes. *Acta Ecol. Sin.* **2005**, *25* (3), 589–595.

(19) Kardinaal, W. E. A.; Visser, P. M. Dynamics of cyanobacterial toxins. In *Harmful Cyanobacteria Aquatic Ecology Series*; Caldwell, M. M., Heldmaier, G., Jackson, R. B., Lange, O. L., Mooney, H. A., Schulze, E.-D., Sommer, U., Eds.; Springer: Dordrecht, the Netherlands, 2005; pp 41–64.

(20) Graneli, E.; Turner, J. T. Ecology of harmful algae. In *Ecological Studies*; Springer: Berlin, Germany, 2006; Vol. 189.

(21) Chorus, I.; Bartram, J. *Toxic Cyanobacteria in Water: A Guide to Their Public Health Consequences, Monitoring and Management*; Spon Press, 1999.

(22) Villareal, T. A. Positive buoyancy in the oceanic diatom *Rhizosolenia debaryana* H. Peragallo. *Deep-Sea Res., Part A* **1988**, *35* (6), 1037–1045.

(23) Milligan, A. J.; Morel, F. M. A proton buffering role for silica in diatoms. *Science* **2002**, *297* (5588), 1848–1850.

(24) Hildebrand, M. Diatoms, biomineralization processes, and genomics. *Chem. Rev.* **2008**, *108* (11), 4855–4874.

(25) Xiong, W.; Yang, Z.; Zhai, H.; Wang, G.; Xu, X.; Ma, W.; Tang, R. Alleviation of high light-induced photoinhibition in cyanobacteria by artificially conferred biosilica shells. *Chem. Commun.* **2013**, *49* (68), 7525–7527.

(26) Xiong, W.; Zhao, X.; Zhu, G.; Shao, C.; Li, Y.; Ma, W.; Xu, X.; Tang, R. Silicification-induced cell aggregation for the sustainable production of H₂ under aerobic conditions. *Angew. Chem.* **2015**, *127* (41), 12129–12133.

(27) Kröger, N.; Lorenz, S.; Brunner, E.; Sumper, M. Self-assembly of highly phosphorylated silaffins and their function in biosilica morphogenesis. *Science* **2002**, *298* (5593), 584–586.

(28) Pohnert, G. Biomineralization in Diatoms Mediated through Peptide- and Polyamine- Assisted Condensation of Silica. *Angew. Chem., Int. Ed.* **2002**, *41* (17), 3167–3169.

(29) Cha, J. N.; Shimizu, K.; Zhou, Y.; Christiansen, S. C.; Chmelka, B. F.; Stucky, G. D.; Morse, D. E. Silicatein filaments and subunits from a marine sponge direct the polymerization of silica and silicines in vitro. *Proc. Natl. Acad. Sci. U. S. A.* **1999**, *96* (2), 361–365.

(30) Kröger, N.; Deutzmann, R.; Bergsdorf, C.; Sumper, M. Species-specific polyamines from diatoms control silica morphology. *Proc. Natl. Acad. Sci. U. S. A.* **2000**, *97* (26), 14133–14138.

(31) Sumper, M.; Lorenz, S.; Brunner, E. Biomimetic Control of Size in the Polyamine-Directed Formation of Silica Nanospheres. *Angew. Chem., Int. Ed.* **2003**, *42* (42), 5192–5195.

(32) Yang, S. H.; Lee, K. B.; Kong, B.; Kim, J. H.; Kim, H. S.; Choi, I. S. Biomimetic encapsulation of individual cells with silica. *Angew. Chem., Int. Ed.* **2009**, *48* (48), 9160–9163.

(33) Ko, E. H.; Yoon, Y.; Park, J. H.; Yang, S. H.; Hong, D.; Lee, K. B.; Shon, H. K.; Lee, T. G.; Choi, I. S. Bioinspired, cyto-compatible mineralization of silica-titania composites: thermoprotective nanoshell formation for individual *Chlorella* cells. *Angew. Chem., Int. Ed.* **2013**, *52* (47), 12279–12282.

(34) Allen, M. M. Simple conditions for growth of unicellular blue-green algae on plates. *J. Phycol.* **1968**, *4* (1), 1–4.

(35) Ma, W.; Shi, D.; Wang, Q.; Wei, L.; Chen, H. Exogenous expression of the wheat chloroplastic fructose-1,6-bisphosphatase gene enhances photosynthesis in the transgenic cyanobacterium, *Anabaena* PCC 7120. *J. Appl. Phycol.* **2005**, *17* (3), 273–280.

(36) Arnon, D. I. Copper enzymes in isolated chloroplasts. Polyphenoloxidase in *Beta vulgaris*. *Plant Physiol.* **1949**, *24* (1), 1–15.

(37) Schreiber, U.; Schliwa, U.; Bilger, W. Continuous recording of photochemical and non-photochemical chlorophyll fluorescence

quenching with a new type of modulation fluorometer. *Photosynth. Res.* **1986**, *10* (1–2), 51–62.

(38) Ma, W.; Wei, L.; Wang, Q. The response of electron transport mediated by active NADPH dehydrogenase complexes to heat stress in the cyanobacterium *Synechocystis* 6803. *Sci. China, Ser. C: Life Sci.* **2008**, *51* (12), 1082–1087.

(39) Kitajima, M.; Butler, W. L. Quenching of chlorophyll fluorescence and primary photochemistry in chloroplasts by dibromothymoquinone. *Biochim. Biophys. Acta, Bioenerg.* **1975**, *376* (1), 105–115.

(40) Geslin, E.; Risgaard-Petersen, N.; Lombard, F.; Metzger, E.; Langlet, D.; Jorissen, F. Oxygen respiration rates of benthic foraminifera as measured with oxygen microsenors. *J. Exp. Mar. Biol. Ecol.* **2011**, *396* (2), 108–114.

(41) Tsapikouni, T.; Garreta, E.; Melo, E.; Navajas, D.; Farré, R. A bioreactor for subjecting cultured cells to fast-rate intermittent hypoxia. *Respir. Physiol. Neurobiol.* **2012**, *182* (1), 47–52.

(42) Chen, W.; Jia, Y.; Li, E.; Zhao, S.; Zhou, Q.; Liu, L.; Song, L. Soil-based treatments of mechanically collected cyanobacterial blooms from Lake Taihu: efficiencies and potential risks. *Environ. Sci. Technol.* **2012**, *46* (24), 13370–13376.

(43) Wei, L.; Li, X.; Yi, J.; Yang, Z.; Wang, Q.; Ma, W. A simple approach for the efficient production of hydrogen from Taihu Lake *Microcystis* spp. blooms. *Bioresour. Technol.* **2013**, *139*, 136–140.

(44) Lin, D. Q.; Brixius, P. J.; Hubbuch, J. J.; Thömmes, J.; Kula, M. R. Biomass/adsorbent electrostatic interactions in expanded bed adsorption: a zeta potential study. *Biotechnol. Bioeng.* **2003**, *83* (2), 149–157.

(45) Lin, D. Q.; Zhong, L. N.; Yao, S. J. Zeta potential as a diagnostic tool to evaluate the biomass electrostatic adhesion during ion-exchange expanded bed application. *Biotechnol. Bioeng.* **2006**, *95* (1), 185–191.

(46) Kosmulski, M.; Prochniak, P.; Rosenholm, J. B. Control of the Zeta Potential in Semiconcentrated Dispersions of Titania in Polar Organic Solvents. *J. Phys. Chem. C* **2009**, *113* (29), 12806–12810.

(47) Hu, H.; Yu, A.; Kim, E.; Zhao, B.; Itkis, M. E.; Bekyarova, E.; Haddon, R. C. Influence of the zeta potential on the dispersability and purification of single-walled carbon nanotubes. *J. Phys. Chem. B* **2005**, *109* (23), 11520–11524.

(48) Chang, H. Y.; Huang, C. C.; Lin, K. Y.; Kao, W. L.; Liao, H. Y.; You, Y. W.; Lin, J. H.; Kuo, Y. T.; Kuo, D. Y.; Shyue, J. J. Effect of surface potential on NIH3T3 cell adhesion and Proliferation. *J. Phys. Chem. C* **2014**, *118* (26), 14464–14470.

(49) Villareal, T. A. Positive buoyancy in the oceanic diatom *Rhizosolenia debaryana* H. Peragallo. *Deep-Sea Res., Part A* **1988**, *35* (6), 1037–1045.

(50) Srivastava, A.; Singh, S.; Ahn, C. Y.; Oh, H. M.; Asthana, R. K. Monitoring approaches for a toxic cyanobacterial bloom. *Environ. Sci. Technol.* **2013**, *47* (16), 8999–9013.

(51) MacKintosh, C.; Beattie, K. A.; Klumpp, S.; Cohen, P.; Codd, G. A. Cyanobacterial microcystin-LR is a potent and specific inhibitor of protein phosphatases 1 and 2A from both mammals and higher plants. *FEBS Lett.* **1990**, *264* (2), 187–192.

(52) Feurstein, D.; Holst, K.; Fischer, A.; Dietrich, D. R. Oatpassaciated uptake and toxicity of microcystins in primary murine whole brain cells. *Toxicol. Appl. Pharmacol.* **2009**, *234* (2), 247–255.

(53) Sengco, M. R.; Anderson, D. M. Controlling harmful algal blooms through clay flocculation. *J. Eukaryotic Microbiol.* **2004**, *51* (2), 169–172.

(54) Liu, Y.; Cao, X.; Yu, Z.; Song, X.; Qiu, L. Controlling harmful algae blooms using aluminum-modified clay. *Mar. Pollut. Bull.* **2016**, *103* (1), 211–219.

(55) Lee, Y. C.; Jin, E.; Jung, S. W.; Kim, Y. M.; Chang, K. S.; Yang, J. W.; Kim, S. W.; Kim, Y. O.; Shin, H. J. Utilizing the algicidal activity of aminoclay as a practical treatment for toxic red tides. *Sci. Rep.* **2013**, *3*, 1292.

(56) Pelaez, M.; Baruwati, B.; Varma, R. S.; Luque, R.; Dionysiou, D. D. Microcystin-LR removal from aqueous solutions using a magneti-

cally separable N-doped TiO₂ nanocomposite under visible light irradiation. *Chem. Commun.* **2013**, 49 (86), 10118–10120.

(57) Moos, N. V.; Bowen, P.; Slaveykova, V. I. Bioavailability of inorganic nanoparticles to planktonic bacteria and aquatic microalgae in freshwater. *Environ. Sci.: Nano* **2014**, 1, 214.

(58) Hamm, C. E.; Merkel, R.; Springer, O.; Jurkojc, P.; Maier, C.; Prechtel, K.; Smetacek, V. Architecture and material properties of diatom shells provide effective mechanical protection. *Nature* **2003**, 421 (6925), 841–843.

(59) Epstein, E. The anomaly of silicon in plant biology. *Proc. Natl. Acad. Sci. U. S. A.* **1994**, 91 (1), 11–17.

(60) Sundar, V. C.; Yablon, A. D.; Grazul, J. L.; Ilan, M.; Aizenberg, J. Fibre-optical features of a glass sponge. *Nature* **2003**, 424 (6951), 899–900.

(61) Walker, J. J.; Spear, J. R.; Pace, N. R. Geobiology of a microbial endolithic community in the Yellowstone geothermal environment. *Nature* **2005**, 434 (7036), 1011–1014.

(62) Neethirajan, S.; Gordon, R.; Wang, L. Potential of silica bodies (phytoliths) for nanotechnology. *Trends Biotechnol.* **2009**, 27 (8), 461–467.